JETIR.ORG ISSN: 2349-5162 | ESTD Year : 2014 | Monthly Issue
JOURNAL OF EMERGING TECHNOLOGIES AND INNOVATIVE RESEARCH (JETIR)
An International Scholarly Open Access, Peer-reviewed, Refereed Journal

Synthetic Polymer–Phytoextract Combinations as Alternative Therapeutics Against Antimicrobial-Resistant Uropathogens Causing Septicemia: An Integrated Experimental and In Silico Investigation

Soham Nashipuri[1], Anirban Mukherjee[2]*

1, Department of Microbiology, Gurudas College, 1/1 Suren Sarkar Road, Beliaghata, Phoolbagan, Kolkata 700054

2, AM Educare Biotech Solutions Pvt Ltd, P-12, CIT Road, Kolkata 700054

*Corresponding author

Abstract

The increasing prevalence of antimicrobial resistance (AMR), driven in part by irrational antibiotic usage, has intensified the incidence of septicemia caused by multidrug-resistant (MDR) urinary tract infection (UTI) pathogens. This study evaluated the antimicrobial potential of two phytochemicals—allicin (*Allium sativum*) and plumbagin (*Plumbago* spp.)—administered alone and in combination with polyethylene glycol (PEG)–citric acid polymeric modulators as a combinatorial therapeutic strategy. Antimicrobial efficacy was assessed using bioassays and time–kill kinetic studies against two natural isolates (Strain A and Strain B). Septicemia-associated effects were examined through micrometric analysis of white blood cell (WBC) morphology in infected human blood samples. Molecular docking simulations targeting the bacterial cytoskeletal protein (PDB ID: 1JCF) were performed to evaluate ligand binding affinity. Strain A exhibited high susceptibility to both phytochemicals, achieving significant growth inhibition within 30–120 min. The PEG–citric acid formulation (1:6 ratio; Polymer 2) enhanced antimicrobial kinetics. In contrast, Strain B demonstrated partial resistance, with transient growth suppression followed by regrowth at 150–210 min. Infection induced marked WBC shrinkage (2.84 µm to 1.72 µm), indicative of septicemic stress, whereas polymer-assisted phytochemical treatment partially restored cellular morphology (2.44 µm). Docking analysis revealed stable ligand–protein interactions, with plumbagin exhibiting lower binding energy and greater thermodynamic stability than allicin. These findings suggest that polymer-modulated phytochemical systems represent a promising alternative strategy against MDR-associated septicemia.

1. Introduction

The persistent emergence of antimicrobial resistance (AMR) has exposed the structural limitations of conventional small-molecule antibiotics, particularly against Multiple Drug Resistant (MDR) uropathogens. These organisms, increasingly encountered in both nosocomial and community-acquired infections, are strongly associated with therapeutic failure and systemic dissemination, especially in resource-limited settings such as India [1,2]. In severe cases, untreated or refractory Urinary Tract Infections (UTIs) progress

to septicemia, a condition characterized by uncontrolled inflammatory cascades, leukocyte structural alterations, oxidative stress imbalance, and multi-organ dysfunction [3,4]. The inability of standard antibiotics to modulate both microbial burden and host immune dysregulation necessitates alternative material-based intervention strategies.

Plants synthesize a wide range of secondary metabolites as biochemical defense mediators against herbivory, oxidative stress, and pathogenic invasion [5,6]. These phytochemicals represent structurally diverse molecular frameworks with redox-active, membrane-reactive, and enzyme-modulating properties, making them promising candidates for antimicrobial development [7]. Nevertheless, their direct clinical translation is often hindered by physicochemical instability, rapid degradation, poor aqueous compatibility, and uncontrolled pharmacokinetics. Integration within a polymeric macromolecular architecture may address these constraints by stabilizing active moieties and modulating release profiles.

The present investigation evaluates two chemically distinct phytochemicals—plumbagin and allicin—against MDR UTI isolates (Strain A and Strain B). Plumbagin (5-hydroxy-2-methyl-1,4-naphthoquinone), isolated from *Plumbago* species [8], possesses a conjugated quinone system capable of redox cycling and intracellular oxidative perturbation, mechanisms implicated in both anticancer and antimicrobial responses [9,10,11]. Allicin (diallylthiosulfinate), derived from *Allium sativum*, is a highly reactive sulfur-containing molecule known to interact with thiol groups of essential microbial enzymes, thereby disrupting metabolic homeostasis in Gram-positive and Gram-negative organisms, including MDR *E. coli* [12,13]. Despite potent bioactivity, both compounds exhibit limited structural persistence under physiological conditions, highlighting the need for a stabilizing matrix.

To overcome these challenges, a synthetic polymer-based modulation platform was designed using Polyethylene Glycol (PEG) in combination with citric acid. PEG is a hydrophilic, flexible polyether widely utilized in biomedical engineering due to its steric stabilization properties, hydration shell formation, and ability to reduce nonspecific protein adsorption [14,15]. While intrinsically non-antimicrobial, PEG provides a molecular backbone capable of supporting conjugation, encapsulation, or intermolecular association with bioactive agents. Citric acid, a multifunctional tricarboxylic acid, contributes additional carboxyl groups that may participate in hydrogen bonding, ionic interactions, or esterification, while also exerting mild antimicrobial effects against the tested strains. The resulting PEG–citric acid system functions as a macromolecular modulator, potentially enhancing phytochemical stability, diffusion behavior, and pathogen–polymer interface interactions.

Chemical validation of phytochemical constituents was conducted using thin-layer chromatography (TLC) coupled with mass spectrometric analysis for functional group confirmation [16]. Complementary qualitative phytochemical assays included the Dragendorff test for alkaloid detection via $[BiI_4]^-$ complex formation, Ferric Chloride testing for tannin-associated iron complexation [17], iodine reactivity for starch identification [18], the Molisch reaction for carbohydrate condensation products [19], and the Ninhydrin assay for amino acid detection through formation of diketohydrindylidene-diketohydrindamine (DYDA) [20]. These procedures ensured compositional accuracy prior to incorporation into the polymeric system.

To elucidate molecular-level interactions within the polymer–phytochemical–pathogen axis, computational simulations were employed. Molecular modeling enables prediction of conformational stability, binding affinity, and non-covalent interaction energies, providing mechanistic insight into how polymer architecture influences bioactive presentation and microbial membrane engagement. Such in silico approaches complement experimental assays by refining hypotheses related to structure–activity relationships and diffusion-mediated effects within hydrated polymer matrices.

In parallel, hematological assessment was performed to examine leukocyte morphological responses (neutrophils, eosinophils, and basophils) under septicemic stress conditions. Micrometric evaluation of

cellular dimensional changes, membrane integrity, and structural distortion offers indirect evidence of inflammatory dysregulation and systemic toxicity [21,22]. Correlating these immune cell parameters with polymer-assisted phytochemical treatment allows evaluation of both antimicrobial efficacy and host compatibility.

Overall, this work proposes a biomacromolecular strategy that integrates redox-active phytochemicals within a PEG–citric acid polymeric framework to counter MDR UTI pathogens and mitigate septicemic progression. By coupling chemical characterization, polymer design, computational modeling, and hematological validation, the study advances a structure-informed approach aligned with current biomaterials research trends focused on multifunctional, biocompatible macromolecular systems for antimicrobial intervention.

2.Materials and methods:

2.1. Selection of Plant Material and Preparation of Phytochemical Extract

Fresh plant materials were selected based on their documented bioactive potential and ethnopharmacological relevance. Rhizomes of *Curcuma longa* (turmeric) and leaves of *Plumbago* spp. were collected and used as sources of phytochemicals. A clinical bacterial isolate (designated Strain A; orange pigment–producing) was employed in subsequent antimicrobial investigations. All chemicals used during extraction were of analytical grade, including methanol, ethanol (99.9%), 70% ethanol, chloroform, acetic acid (Merck Life Science Pvt. Ltd., India), and distilled water.

Plant materials were thoroughly cleaned and mechanically processed to obtain a fine homogenized paste using separate mortar and pestle sets to avoid cross-contamination between samples. The homogenized plant mass was extracted using a methanol–water solvent system, with the solvent volume adjusted to approximately half the working capacity of the mortar. The mixture was transferred into 50 mL glass beakers and subjected to controlled extraction under continuous stirring using a magnetic stirrer equipped with a heating plate. Mild heating was applied intermittently to facilitate solvent penetration and phytochemical dissolution while preventing solvent boiling or thermal degradation of bioactive compounds.

The extraction process was continued until the total volume was reduced to approximately 50% of the initial volume (typically from 50 mL to ~25 mL), ensuring concentration of the phytochemical constituents. The concentrated extracts were then transferred into sterile 2 mL microcentrifuge tubes, sealed with parafilm to prevent solvent evaporation, appropriately labeled, and stored at 4 °C until further physicochemical and biological analysis.

2.2. Isolation of strains: Natural isolates were isolated from pond water with the help of Hichrome UTI chromogenic medium (Himedia, India) and later it was identified as per manufacturer's manual. Isolated natural isolates were named as Strain A and Strain B on the basis of their different colour of colony on UTI agar. Isolates were further subcultured in nutrient broth and preserved at 4^{o}C for further analysis.

2.3. Thin layer chromatography (TLC) for the phytochemicals (plumbagin, allicin, and curcumin): Different solvent systems were used to identify bioactive components of crude phyto extract. Briefly, for the solvent or the mobile phase, two types of sample were prepared, a polar solvent and a non polar solvent. For the polar solvent, chloroform is mixed with ethanol, and acetic acid in the ratio of 90:5:1 and for the non-polar solvent the ratio of n-hexane : methanol : chloroform was 4:10:49 respectively. Supplied TLC plates of a length of 7-8 cm long and about 4cm thick were taken for spotting with the help of glass capillary. A line was drawn with a pencil about 1cm up from the base, and spots were made. The solvents were placed in a beaker and the TLC plates were put vertically inside so that the solvent immersed the plate just up to the

pencil line and touched the dots. The setup was left for some time at room temperature and then was taken out, put for 20 seconds in the incubator at 37ºC for drying observed under visible light and UV light.

2.4.Chemical analysis of phytochemicals: Biochemical characterization of the phytochemical samples was conducted through a series of qualitative assays to identify their primary and secondary metabolites. For the detection of alkaloids, the sample was treated with Dragendorff reagent (potassium bismuth iodide), where the formation of a colored precipitate indicated the reaction of alkaloid groups to form an aromatic compound and $[BiI4]^-$. Tannin and phenolic content were assessed using a freshly prepared 5% $FeCl_3$ solution; the reaction of Fe^{3+} ions with tannins produced unstable colored rings or precipitates through the formation of tannin-iron bis and tris complexes [17]. Starch presence was determined by the addition of iodine, which reacts with colloidal starch to form starch iodide, imparting a characteristic bluish color due to the high absorptive properties of the colloid [18]. The Molisch test was utilized for carbohydrate detection, where the addition of H_2SO_4 and alpha-naphthol led to the formation of a bluish-violet condensed product from the furfural or hydroxymethylfurfural derivatives of pentoses and hexoses [90]. Finally, the Ninhydrin test was performed to identify amino acids; this process involved the oxidative deamination of amino acids to form ammonia and the reduction of ninhydrin to hydrindantin, which subsequently condensed with ammonia to produce the purple-colored anion diketohydrindylidene-diketohydrindamine (DYDA) [20].

2.5. Preparation of polymer 1 and 2: Dilutions were made with 2 different supplied polymers such as 1 and 2 in the ratio 1:5 and 1:6 respectively. Stock solutions of 1% for both of the polymers were made by adding 10 ml water for both the polymer mixes. Now serial dilutions were made of polymer 1 and 2. For both the polymers, 4 falcon tubes were taken. 1 was kept for the stock, the rest 3 for serial dilutions. In the 3 test tubes, 5 ml of water was added, the rest 5 ml were added from the serial dilutions. From stock, 5 ml water was added to the tube 1 and 5 ml water was added (5% concentration). From tube 1, 5ml was added to tube 2 and 5 ml water was added (2.5% concentration). From tube 2, 5ml was added to tube 3 and 5ml water was added (1.25% concentration).

2.6.Cup plate assay: Nutrient agar was prepared in accordance with the standard instructions provided by the manufacturer's instruction. Briefly, the agar was melted, secured with a cotton plug, wrapped in paper, and sterilized via autoclaving. Once the sterilization process was completed, 20 ml of the molten agar was poured into each petri dish already inoculated with 0.2 ml of respective strains, mixed well and left undisturbed for 15 minutes to allow for complete solidification. After the medium had set, a sterile borer was used to create wells extending to the bottom of the plate, with either two or four bores made per dish depending on the specific test requirements. Finally, a volume of 100 µl samples were dispensed into each well for analysis and kept at 37ºC for overnight incubation.

2.7.Growth Curve Determination of bacterial strains: Luria broth was prepared in nephalometric flasks and sterilized via autoclaving. Following sterilization, the medium was inoculated with a 1.5% (v/v) bacterial culture, corresponding to 1.5 ml of culture per 100 ml of broth. Treatment groups were established by adding 1.5% phytochemicals directly to the flasks. For the experimental groups involving phytochemicals combined with modulators (specifically Polymer 1 and Polymer 2), mixtures containing 1.5% of the respective phytochemicals and modulator were prepared separately in sterile Falcon tubes. Finally, these prepared mixtures and the cellular inocula were added to the Luria broth in the nephalometric flasks to initiate the assay.

After adding all the components in the flasks, the flask was kept at 37°C in BOD incubator cum shaker, and measured the optical density in a colorimeter at 620 nm at an interval of every 30 minutes

2.8.Septicaemia determination of blood:

Human blood was kept in an EDTA vial at refrigerated condition. The blood was mixed with the strains in an Eppendorff tube seeded with the phytochemicals and modulators at a ratio of 1:1. Finally, treated samples were also smeared, stained with leishman stain.All the slides were observed along with the control (untreated) slide to observe under a compound microscope at 45x and 100x magnification. The sizes of the WBCs are measured through micrometry at respective magnification.

2.9.Computational Characterization and analysis: Bioinformatics tools like discovery studios, autodock.bat., chem, chimera X, graphpad prism 8, pmv-1.5.7, racoon VS-1.5.7, vision-1.5.7, Ray for windows were used to simulate molecular docking of samples against cytoskeleton protein of target natural isolates. Here the cytoskeletal protein 1jcf, an MreB protofilament, was found from the protein data base (pdb) and the binding of the molecules allicin and plumbagin were checked for 100 cycles run in the docking software.

3. Results:

3.1.Thin layer chromatography (tlc) of phytochemicals:

TLC analysis of curcumin revealed three bands—**curcumin**, **desmethoxycurcumin**, and **bisdesmethoxycurcumin**—separated by their solubility in the mobile phase. Curcumin, the most soluble, traveled the greatest distance (**6.5 cm**), followed by desmethoxycurcumin (intermediate), and bisdesmethoxycurcumin (shortest), a pattern that remained consistent across different runs. Plumbagin analysis identified three sub-pigments: **Pigment 1** (highest solubility/Rf) traveled **4.3 cm** in a polar solvent, followed by the plumbagin core and **Pigment 2** (lowest solubility). Notably, the plumbagin core showed nearly equal solubility in both polar and non-polar systems (**2.5 cm**), maintaining the same relative migration order. These isolated phytochemical subparts are now ready for further detailed testing.

Table 1: TLC analysis of curcumin and plumbagin. All of the data is recorded in centimetres.

Pigment	Solvent	Difference of dots (cm)	Rf values
1. Curcumin	Polar	5	0.762
2.Desmethoxy curcuminoid	Polar	4.1	0.630
3.Bisdesmethoxy curcuminoid	Polar	3.6	0.553
1. Curcumin	Non Polar	5	0.762
2.Desmethoxy curcuminoid	Non Polar	4.1	0.630
3.Bisdesmethoxy curcuminoid	Non Polar	3.6	0.553
1. Pigment-1	Polar	2.9	0.68
2. Plumbagin	Polar	3.4	0.8
3. Pigment-2	Polar	3.8	0.88
4. Pigment-1	Non Polar	1.7	0.68
5. Plumbagin	Non Polar	2	0.80
6. Pigment-2	Non Polar	2.2	0.88

3.2.Biochemical Test: Allicin tested positive for alkaloids, ninhydrin-reactive compounds (proteins/amino acids), and the Molisch test (carbohydrates), while showing negative results for tannins and starch. Conversely, plumbagin tested positive for tannins and starch but yielded negative results for alkaloids, ninhydrin-reactive compounds, and the Molisch test. These results indicate that allicin is characterized by a high presence of nitrogenous compounds and carbohydrates, whereas plumbagin is primarily associated with polyphenolic tannins and storage polysaccharides.

3.3. Cup plate assay: In the antimicrobial assessment of various modulators and phytochemicals, the sensitivity profiles of Strain A and Strain B were systematically evaluated. Initial tests on modulator sets revealed that while both strains were insensitive to the 1:5 PEG-Citric acid polymer, they exhibited sensitivity to the 1:6 ratio, with Strain B showing a larger zone of inhibition (1.8 cm) compared to Strain A (1.2 cm). Regarding solvent effects, both strains remained unaffected by aqueous extracts; however, methanolic extracts of allicin and plumbagin demonstrated cidal activity against Strain A, while only the methanolic allicin extract was effective against Strain B. Although methanol itself showed a minor inhibitory effect (0.5 cm) on Strain A, it was completely inactive against Strain B, justifying its use as a solvent for subsequent combination assays.

In the combination assays involving allicin and various polymer concentrations, Strain A remained entirely insensitive to all tested dilutions of both Polymer 1 and Polymer 2. In contrast, Strain B exhibited sensitivity to the 10% concentration of the allicin-Polymer 2 mixture and demonstrated susceptibility to both the 10% and 5% concentrations of the allicin-Polymer 1 mixture. When testing plumbagin combinations, Strain A showed significant sensitivity specifically to the lower concentrations (2.5% and 1.25%) of the Polymer 1 mixture, with no inhibition observed at higher concentrations or with any Polymer 2 combinations. Strain B was found to be completely insensitive to all tested concentrations of plumbagin combined with either polymer. These findings identify specific effective concentrations of allicin-polymer and plumbagin-polymer combinations that are suitable for further Minimum Inhibitory Concentration (MIC) studies against these UTI pathogens.

3.4. Growth curve analysis of strains:

The growth kinetics of Strain A and Strain B were systematically evaluated to determine the antimicrobial efficacy of allicin and plumbagin, both independently and in coordination with polymeric modulators. Control groups for both strains exhibited characteristic sigmoidal growth profiles, transitioning through distinct lag, log, and stationary phases, thereby confirming the baseline viability of the experimental cultures. For Strain A, the introduction of allicin and plumbagin resulted in immediate and sustained growth inhibition, with optical density (OD) remaining constant throughout the observation period. Notably, the combination of these phytochemicals with Polymer 2 appeared to accelerate the cidal effect, achieving total suppression within 30 minutes of inoculation. This suggests a potent synergistic interaction where the polymer enhances the bioavailability or membrane-permeabilizing capabilities of the phytochemicals against sensitive strains.

In contrast, the susceptibility of Strain A was significantly altered when plumbagin was administered in conjunction with Polymer 1. While plumbagin alone effectively inhibited the strain, the combination treatment allowed for a gradual rise in optical density after the 210-minute mark. This phenomenon indicates a possible antagonistic interaction or a competitive suppression mechanism, where Polymer 1 may sequester the active plumbagin molecules, effectively reducing their concentration below the Minimum Inhibitory Concentration (MIC). Conversely, when allicin was paired with Polymer 1, the inhibitory effect remained absolute, suggesting that the allicin-Polymer 1 complex either maintains high antimicrobial stability or that the intrinsic potency of allicin is sufficient to override any potential modulatory interference in Strain A.

The experimental results for Strain B revealed a robust resistance profile, sharply contrasting with the sensitivity observed in Strain A. Although the application of allicin and plumbagin initially induced a slight delay in proliferative activity, Strain B consistently overcame these antimicrobial challenges. In all instances involving allicin—whether administered alone or with polymeric modulators—the culture initiated a steady growth phase after approximately 210 minutes. This suggests that Strain B possesses an inherent physiological response system, such as efflux pump activation or enzymatic degradation, capable of neutralizing the phytochemical. The lack of sustained inhibition by the polymer-allicin mixtures further

indicates that these modulators were unable to bypass the strain's defense mechanisms, resulting in a proliferative phase that mirrored the healthy control.

Further analysis of plumbagin treatments on Strain B confirmed a similar pattern of resistance and recovery. Despite an initial period of slow growth, the strain exhibited a significant surge in optical density at the 150-minute interval across all plumbagin-based experimental groups. The observation that Polymer 1 and Polymer 2 failed to prevent this recovery supports the conclusion that Strain B is highly resilient to these specific phytochemical interventions. Additionally, individual testing of the polymers confirmed they possess no intrinsic antimicrobial properties, as cultures treated solely with Polymer 1 or Polymer 2 returned to standard growth trajectories following a brief lag phase. Consequently, while these phytochemical-polymer combinations show promise for treating sensitive pathogens, their efficacy is strictly limited by the rapid adaptive response and neutralising capacity of resistant strains like Strain B.

Table2: Growth curve for Strain A with allicin and modulator

Time In Minutes	Strain A Control	Strain A Control with allicin	Strain A Control With allicin and polymer 1	Strain A Control With allicin and polymer 2	Strain A With Polymer-1	Strain A With Polymer-2
0	0.01	0.06	0.02	0.05	0	0.01
30	0.02	0.07	0.02	0.05	0	0.02
60	0.03	0.09	0.02	0.05	0.01	0.03
90	0.05	0.09	0.02	0.05	0.05	0.09
120	0.07	0.10	0.02	0.05	0.27	0.31
150	0.11	0.12	0.02	0.05	0.47	0.5
180	0.19	0.12	0.02	0.06	0.62	0.64
210	0.30	0.10	0.02	0.06	0.69	0.71
240	0.44	0.10	0.02	0.06	0.76	0.76
270	0.54	0.10	0.02	0.06		
300	0.60	0.10	0.02	0.06		
330	0.66	0.09	0.02	0.06		

Table 3: Growth curve for Strain A with Plumbagin and modulator						
Time In Minutes	Strain A Control	Strain A Control with Plumbagin	Strain A Control With Plumbagin and polymer 1	Strain A Control With Plumbagin and polymer 2	Strain A With Polymer-1	Strain A With Polymer-2
0	0.01	0.10	0.05	0.06	0	0.01
30	0.02	0.11	0.05	0.06	0	0.02
60	0.03	0.11	0.08	0.06	0.01	0.03
90	0.05	0.11	0.10	0.06	0.05	0.09
120	0.07	0.11	0.11	0.05	0.27	0.31
150	0.11	0.12	0.12	0.05	0.47	0.5
180	0.19	0.12	0.12	0.05	0.62	0.64
210	0.30	0.12	0.16	0.05	0.69	0.71
240	0.44	0.12	0.31	0.05	0.76	0.76
270	0.54	0.12	0.39	0.06		
300	0.60	0.12	0.53	0.06		
330	0.66	0.12	0.60	0.06		

Table 4: Growth curve for Strain B with Allicin and modulator						
Time In Minutes	Strain B Control	Strain B Control with Allicin	Strain B Control With Allicin and polymer 1	Strain B Control With Allicin and polymer 2	Strain B With Polymer-1	Strain B With Polymer-2
0	0.01	0.01	0.03	0.02	0.01	0.01
30	0.02	0.06	0.03	0.03	0.01	0.01
60	0.03	0.07	0.03	0.05	0.01	0.01
90	0.04	0.08	0.03	0.05	0.01	0.03
120	0.06	0.08	0.04	0.06	0.03	0.06
150	0.13	0.08	0.05	0.06	0.07	0.1
180	0.26	0.08	0.06	0.08	0.17	0.19
210	0.40	0.11	0.12	0.13	0.3	0.34
240	0.52	0.12	0.26	0.19	0.46	0.46
270	0.60	0.18	0.34	0.27		
300	0.67	0.25	0.45	0.32		
330	0.73	0.35	0.53	0.37		

Table 5: Growth curve for Strain B with Plumbagin and modulator						
Time In Minutes	Strain B Control	Strain B Control with Plumbagin	Strain B Control With Plumbagin and polymer 1	Strain B Control With Plumbagin and polymer 2	Strain B With Polymer-1	Strain B With Polymer-2
0	0.01	0.10	0.06	0.03	0.01	0.01
30	0.02	0.13	0.06	0.03	0.01	0.01
60	0.03	0.14	0.06	0.03	0.01	0.01
90	0.04	0.15	0.06	0.03	0.01	0.03
120	0.06	0.15	0.08	0.07	0.03	0.06
150	0.13	0.16	0.15	0.12	0.07	0.1
180	0.26	0.17	0.18	0.22	0.17	0.19
210	0.40	0.19	0.23	0.34	0.3	0.34
240	0.52	0.23	0.36	0.48	0.46	0.46
270	0.60	0.36	0.42	0.53		
300	0.67	0.54	0.58	0.64		
330	0.73	0.64	0.62	0.69		

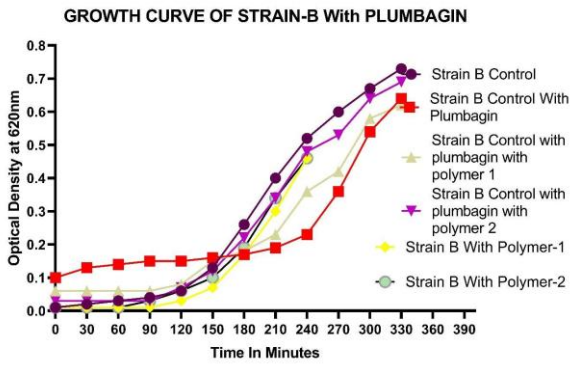

Fig 1a)

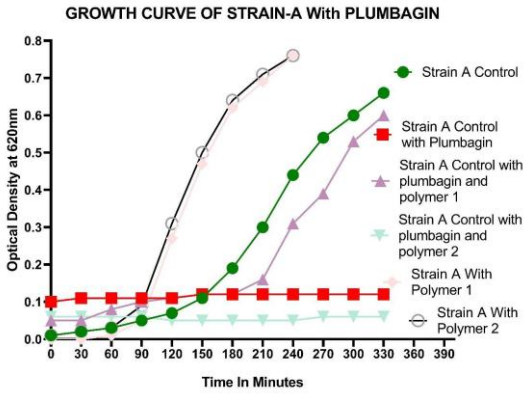

Fig 1b)

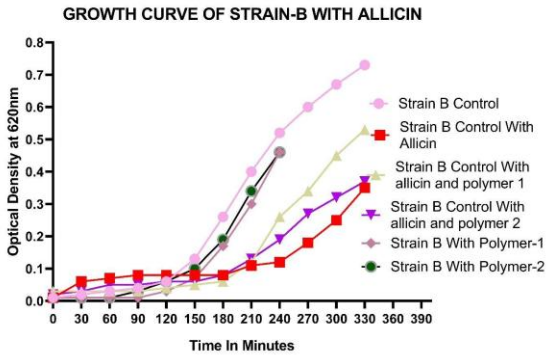

Fig 1c)

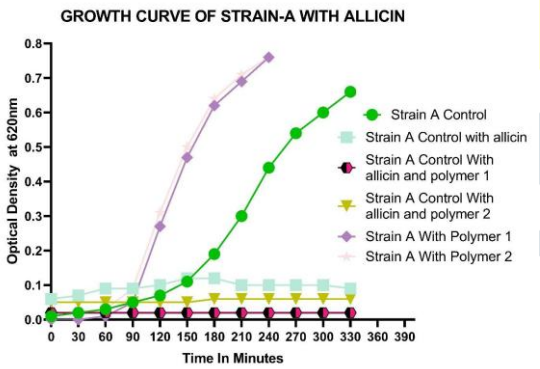

fig 1d)

Fig 1: Growth curve of bacrerial strain isolates A and B .a) plumbagin with moulators for strain B , b) plumbagin with modulators for strain A, c) allicin with modulators for strain B, d) allicin with modulators for strain A

3.5.WBC micrometry of blood samples: The physiological impact of microbial infection on host immune cells was evaluated through micrometric analysis of White Blood Cells (WBCs) in various experimental conditions. In a controlled, healthy blood sample, the leukocytes exhibited a standard average diameter of 2.84 µm. This baseline measurement serves as a reference point for identifying morphological changes induced by the introduction of

pathogenic strains, specifically Strain A and Strain B. These measurements are critical in understanding the cellular-level response to septicemic stress, where changes in cell volume often correlate with the severity of the inflammatory or toxic response.

Upon infection with the bacterial strain infection models, a significant reduction in leukocyte diameter was observed, indicating a state of cellular shrinkage or "septic shock." The blood sample infected with Strain A showed the most drastic reduction in cell size, with an average diameter of 1.72 µm. Infection with Strain B also resulted in a marked decrease in WBC size to an average of 1.87 µm. This reduction in diameter suggests that Strain A exerts a more potent cytotoxic effect on the host immune cells compared to Strain B, potentially through more aggressive oxidative mechanisms or higher rates of cytosolic material loss.

To assess the potential for therapeutic intervention, a modulator—Polymer 2—was introduced into the Strain B infection model. The selection of Polymer 2 was based on its superior antibacterial performance observed in previous cup-plate assays. Micrometric analysis revealed that the addition of the modulator successfully mitigated the degree of cellular shrinkage; the average WBC diameter in the Strain B + Modulator group increased to 2.44 µm. While this value remains lower than that of the healthy control, it represents a substantial recovery compared to the unmodulated Strain B sample.

The comparative results indicate that the size of WBCs is consistently larger in healthy or modulated blood samples than in those subjected to raw bacterial infection. The ability of Polymer 2 to partially restore leukocyte morphology suggests that the modulator effectively inhibits the cidal mechanisms of the bacteria, thereby protecting the white blood cells from the full extent of septicemic degradation. These findings provide a foundational understanding of how specific polymers may be utilized to reduce the physiological impact of septic shock and enhance host cell resilience during systemic infection

3.6.Bioinformatics analysis: For the bioinformatics analysis, The protein 1JCF was actually common for both strain A and strain B. The binding spots for the protein for allicin and plumbagin were found by molecular docking, and the results were obtained. Following 100 cycles, AutoDockTools displayed the lowest binding energies for both plumbagin and allicin, with amino acids shown and linked with numerous bonds.

Despite using different chemical dynamics, molecular docking results show that allicin and plumbagin both exhibit strong binding affinities for the bacterial cytoskeletal protein 1jcf. Allicin's hydrophobicity and reactive sulphur groups enable efficient anchoring within the protein scaffold, while plumbagin's naphthoquinone structure achieves a highly stable configuration. The molecule with the more negative value creates a stronger and more spontaneous interaction when their lowest binding energies (kcal/mol) are compared. These results ultimately imply that both phytochemicals function as competitive inhibitors of 1JCF, which may halt bacterial cell division and offer a strong two-pronged approach to combating infections that are resistant to multiple drugs.
Comparative molecular docking analysis indicates that plumbagin possesses a superior binding affinity for the bacterial cytoskeletal protein 1jcf relative to allicin. This enhanced affinity is attributed to the distinct thermodynamic profiles and structural characteristics of the two ligands. Plumbagin, a naphthoquinone, features a rigid, planar aromatic framework that facilitates stable hydrophobic interactions and π-stacking within the 1JCF binding pocket.

These interactions culminate in a significantly lower (more negative) binding energy, reflecting a highly spontaneous and robust protein-ligand association.

Conversely, while allicin exhibits potent reactivity toward thiol groups, its flexible aliphatic chain and lower molecular weight yield a comparatively higher (less negative) binding energy. Consequently, in a competitive binding environment for the 1JCF active site, plumbagin is predicted to function as the more potent inhibitor. Nevertheless, both phytochemicals demonstrate significant potential as antimicrobial agents, utilizing independent biochemical mechanisms to combat multidrug-resistant bacterial strains.

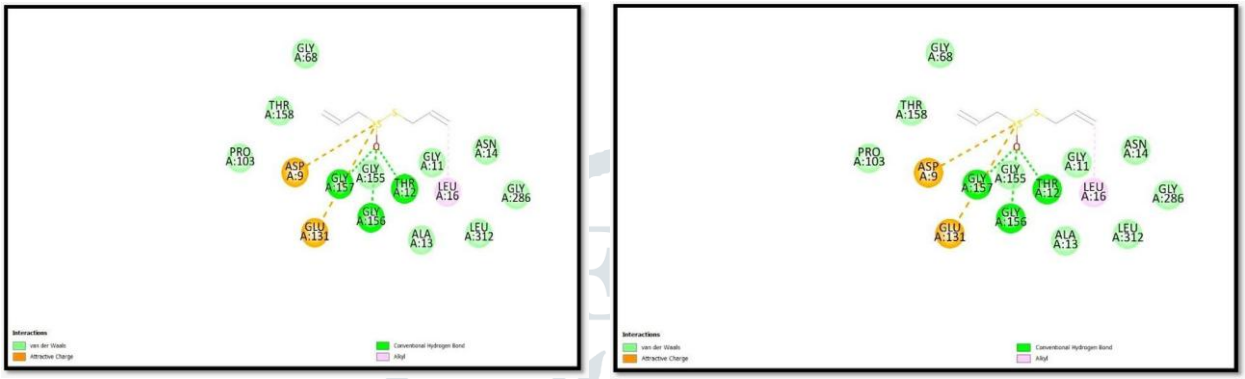

Fig 2a) fig 2b)

Fig 2: bioniformatics analysis and establishing lowest binding energy conformer showing cytoskeletal protein 1jcf and a) allicin , b)plumbagin

4.Discussion:

Chromatographic analysis of the plant extracts revealed the chemically heterogeneous nature of the phytochemical fractions used in this study. Separation of the curcuminoid extract yielded three distinguishable bands corresponding to curcumin, desmethoxycurcumin, and bisdesmethoxycurcumin, demonstrating the well-known compositional diversity of curcuminoid complexes. The comparable Rf values obtained under both polar and non-polar solvent systems indicate that these derivatives possess relatively consistent partitioning behaviour, suggesting similar polarity characteristics. In the plumbagin extract, additional minor pigment bands were also observed alongside the principal compound. These secondary components may arise from co-extracted metabolites or environmental variations affecting plant biosynthesis. Such compositional complexity is important because the biological activity of crude phytochemical extracts often depends on synergistic or antagonistic interactions among the constituent molecules rather than the action of a single compound.

Qualitative biochemical assays further highlighted the chemical differences between the investigated phytochemicals. Allicin showed positive responses in tests associated with nitrogenous or reactive functional groups, which is consistent with its biosynthesis from sulfur-containing amino acid derivatives and its well-known reactivity with cellular thiol groups. In contrast, plumbagin demonstrated reactions typical of polyphenolic or quinone-type molecules. These differences suggest distinct antimicrobial mechanisms. Allicin likely exerts its activity through disruption of protein function and oxidative stress induction, whereas plumbagin, owing to its naphthoquinone structure, may interfere with cellular redox balance and structural proteins involved in bacterial metabolism.

Antimicrobial assays revealed notable differences between the two environmental isolates tested. Strain A exhibited greater susceptibility to the phytochemical extracts, particularly in methanolic preparations, while Strain B displayed a comparatively resistant phenotype, especially toward plumbagin. The incorporation of PEG–citric acid polymer (1:6 ratio) significantly increased the observed inhibition zones, indicating that the polymer system enhanced the bioavailability or delivery efficiency of the phytochemicals. Methanol alone produced minimal inhibition, confirming its suitability as a neutral extraction solvent rather than an antimicrobial agent. Interestingly, Strain B demonstrated partial sensitivity when treated with specific allicin–polymer combinations, suggesting that the polymer matrix may facilitate improved penetration of the phytochemical through the bacterial envelope.

Growth-kinetic experiments provided additional insight into the nature of the antimicrobial response. Rapid growth suppression of Strain A within the first 30 minutes in the presence of Polymer 2 suggests strong synergistic activity between the polymer carrier and the phytochemical agents. However, delayed regrowth of Strain A in the plumbagin–Polymer 1 treatment group after prolonged incubation may indicate antagonistic interactions, possibly resulting from excessive polymer–drug association that limits the availability of free plumbagin molecules. In contrast, the recovery of Strain B after 150–210 minutes across most treatments suggests the activation of adaptive defense mechanisms such as efflux systems or enzymatic detoxification.

Micrometric examination of human blood samples provided evidence of pathogen-induced cellular stress. Infection with the bacterial isolates resulted in a marked reduction in white blood cell (WBC) diameter, indicating cellular shrinkage associated with septicemic stress. Interestingly, treatment with polymer-phytochemical combinations partially restored WBC morphology, suggesting a protective effect that may arise from reduced bacterial toxicity or stabilization of cellular membranes. This observation highlights the potential dual role of polymer-assisted phytochemical systems in both antimicrobial activity and host cell protection.

Molecular docking studies supported the experimental observations by identifying potential interactions between the phytochemicals and the bacterial cytoskeletal protein (PDB ID: 1JCF), which plays an important role in cell division. Both allicin and plumbagin demonstrated favorable binding within the protein pocket. However, plumbagin exhibited a more negative binding energy, indicating stronger interaction and greater thermodynamic stability. The planar naphthoquinone structure of plumbagin may facilitate stable stacking interactions within the active site, whereas the flexible aliphatic structure of allicin may contribute to comparatively weaker binding stability.

Overall, the findings demonstrate that phytochemical–polymer systems can exert significant antimicrobial effects against susceptible bacterial isolates while also influencing host cellular responses. Among the tested compounds, plumbagin showed particularly promising activity due to its favorable molecular interactions and structural stability. Future investigations should focus on optimizing polymer–phytochemical ratios and delivery strategies, as well as expanding screening to a broader range of resistant pathogens. Such integrated approaches may contribute to the development of alternative antimicrobial therapies capable of addressing the growing global challenge of multidrug resistance.

5.References and citations:

[1]Elshobary ME, Badawy NK, Ashraf Y, Zatioun AA, Masriya HH, Ammar MM, Mohamed NA, Mourad S, Assy AM. Combating antibiotic resistance: mechanisms, multidrug-resistant pathogens, and novel therapeutic approaches: an updated review. Pharmaceuticals. 2025 Mar 12;18(3):402.

[2] Van Duin D, Paterson D. Multidrug resistant bacteria in the community: trends and lessons learned. Infectious disease clinics of North America. 2016 Jun;30(2):377.

[3] Cheng L, Cao Y, Liu S, Lv L, Zhang J, Bao J, Wang G, Xu P. Unveiling the research advances of sepsis: pathogenesis, precise intervention and clinical perspective. International Journal of Surgery. 2025 Sep 1;111(9):6260-89.

[4] Srdić T, Đurašević S, Lakić I, Ružičić A, Vujović P, Jevđović T, Dakić T, Đorđević J, Tosti T, Glumac S, Todorović Z. From molecular mechanisms to clinical therapy: understanding sepsis-induced multiple organ dysfunction. International journal of molecular sciences. 2024 Jul 16;25(14):7770.

[5] Upadhyay R, Saini R, Shukla PK, Tiwari KN. Role of secondary metabolites in plant defense mechanisms: A molecular and biotechnological insights. Phytochemistry Reviews. 2025 Feb;24(1):953-83.

[6] Al-Khayri JM, Rashmi R, Toppo V, Chole PB, Banadka A, Sudheer WN, Nagella P, Shehata WF, Al-Mssallem MQ, Alessa FM, Almaghasla MI. Plant secondary metabolites: the weapons for biotic stress management. Metabolites. 2023 May 31;13(6):716.

[7]Patra AK. An overview of antimicrobial properties of different classes of phytochemicals. Dietary phytochemicals and microbes. 2012 Feb 18:1-32.

[8] Sand JM, Hafeez BB, Jamal MS, Witkowsky O, Siebers EM, Fischer J, Verma AK. Plumbagin (5-hydroxy-2-methyl-1, 4-naphthoquinone), isolated from Plumbago zeylanica, inhibits ultraviolet radiation-induced development of squamous cell carcinomas. Carcinogenesis. 2012 Jan 1;33(1):184-90.

[9] Padhye S, Dandawate P, Yusufi M, Ahmad A, Sarkar FH. Perspectives on medicinal properties of plumbagin and its analogs. Medicinal research reviews. 2012 Nov;32(6):1131-58.

[10]Kavi Kishor PB, Thaddi BN, Guddimalli R, Nikam TD, Sambasiva Rao KR, Mukhopadhyay R, Singam P. The Occurrence, Uses, Biosynthetic Pathway, and Biotechnological Production of Plumbagin, a Potent Antitumor Naphthoquinone. Molecules. 2025 Apr 4;30(7):1618.

[11] Yin Z, Zhang J, Chen L, Guo Q, Yang B, Zhang W, Kang W. Anticancer effects and mechanisms of action of plumbagin: review of research advances. BioMed Research International. 2020;2020(1):6940953.

[12] Bhatwalkar SB, Mondal R, Krishna SB, Adam JK, Govender P, Anupam R. Antibacterial properties of organosulfur compounds of garlic (Allium sativum). Frontiers in microbiology. 2021 Jul 27;12:613077.

[13] Borlinghaus J, Foerster J, Kappler U, Antelmann H, Noll U, Gruhlke MC, Slusarenko AJ. Allicin, the odor of freshly crushed garlic: A review of recent progress in understanding allicin's effects on cells. Molecules. 2021 Mar 10;26(6):1505.

[14] D'souza AA, Shegokar R. Polyethylene glycol (PEG): a versatile polymer for pharmaceutical applications. Expert opinion on drug delivery. 2016 Sep 1;13(9):1257-75.

[15] Parray ZA, Hassan MI, Ahmad F, Islam A. Amphiphilic nature of polyethylene glycols and their role in medical research. Polymer Testing. 2020 Feb 1;82:106316.

[16]Kowalska T, Sajewicz M. Thin-layer chromatography (TLC) in the screening of botanicals–its versatile potential and selected applications. Molecules. 2022 Oct 5;27(19):6607.

[17]Narasimhan Sreevidya NS, Shanta Mehrotra SM. Spectrophotometric method for estimation of alkaloids precipitable with Dragendorff's reagent in plant materials.

[18] Manion BA, Holbein BE, Marcone MF, Seetharaman K. A new method for quantifying iodine in a starch–iodine matrix. Carbohydrate research. 2010 Dec 10;345(18):2698-704.

[19] Lamothe PJ, McCormick PG. Role of hydrindantin in the determination of amino acids using ninhydrin. Analytical Chemistry. 1973 Sep 1;45(11):1906-11.

[20] Ahmed I, Balestrieri E, Tudosa I, Lamonaca F. Morphometric measurements of blood cell. Measurement: Sensors. 2021 Dec 1;18:100294.

[21] Tvedten H, Raskin RE. Leukocyte disorders. Small animal clinical diagnosis by laboratory methods. 2011 Dec 15:63.

[22] Bainton DF. Morphology of neutrophils, eosinophils, and basophils. Williams hematology. 1995 May;5:753-65.